

Helium impurity ion densities measured with Lithium beam charge exchange spectroscopy

E. Wolfrum, J. Schweinzer, M. Reich, R. Dux and the ASDEX Upgrade Team

Max Planck Institut für Plasmaphysik, EURATOM Association, Garching, Germany

Introduction

Glow discharges in helium are used as standard machine conditioning procedure at the ASDEX Upgrade tokamak. As a consequence, helium released from the wall during a plasma discharge is a viable candidate for impurity charge exchange (CX) measurements. The method of lithium beam CX spectroscopy has been used for the density measurement of He^{2+} impurity ions at the plasma edge¹.

Experimental setup

The isotopically pure ${}^7\text{Li}$ ions are extracted from a β -eucryptite emitter, accelerated to the chosen energy and subsequently neutralised via charge exchange in a sodium vapour cell. In the measurements presented here, the Lithium beam energy was always set to 40 keV, optimising the charge exchange cross sections and neutralisation efficiency but compromising beam penetration into the plasma. With these settings the beam delivers a neutral beam equivalent current of about 2.2 mA within a diameter of 10-15 mm. The beam is chopped by means of horizontal deflection plates positioned between ion source and neutraliser cell with a beam on:off cycle of 56:24 ms. A schematic view of the position of the lithium beam and its optical systems is shown in figure 1.

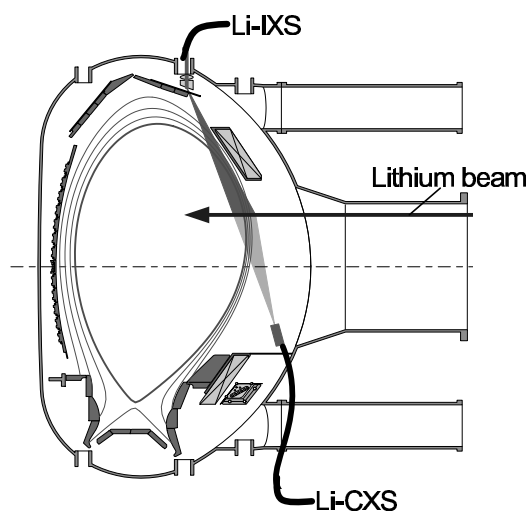


Figure 1: Schematic view of the Lithium beam and its optical systems:

Li-IXS (Lithium beam impact excitation spectroscopy): 35 lines of sight (LOS) equipped with a filter-photomultiplier detection system.

Li-CXS (Lithium beam charge exchange spectroscopy): 18 LOS connected to two 0.75 m Czerny Turner spectrometers (1200 l/mm gratings) with frame transfer CCDs.

The Lithium beam is chopped so that the active charge exchange signal is determined by subtraction of an averaged background of the temporally neighbouring ‘beam off’-measurements from the ‘beam on’-measurements.

He^{2+} densities and temperatures² can be measured in H-modes only in between ELMs by disregarding CCD camera frames which contain ELM induced signals. Figures 2a and 2b show measured spectra of the He II (3-4) charge exchange line at 468.57 nm, taken in an L-mode and in an ELMy H-mode plasma discharge, respectively. There is a clear error maximum in the centre of the He II line due to the very large but spectrally narrow He II background radiation. In figure 2b it can clearly be seen that in the region of the large error bars the data are not statistically distributed within the range of these error bars. This is due to the nature of the background, namely He^+ density fluctuations following ELMs. These fluctuations lead to strongly varying intensities of the cold He II background line and subsequently to the observed pixel-to-pixel correlated noise.

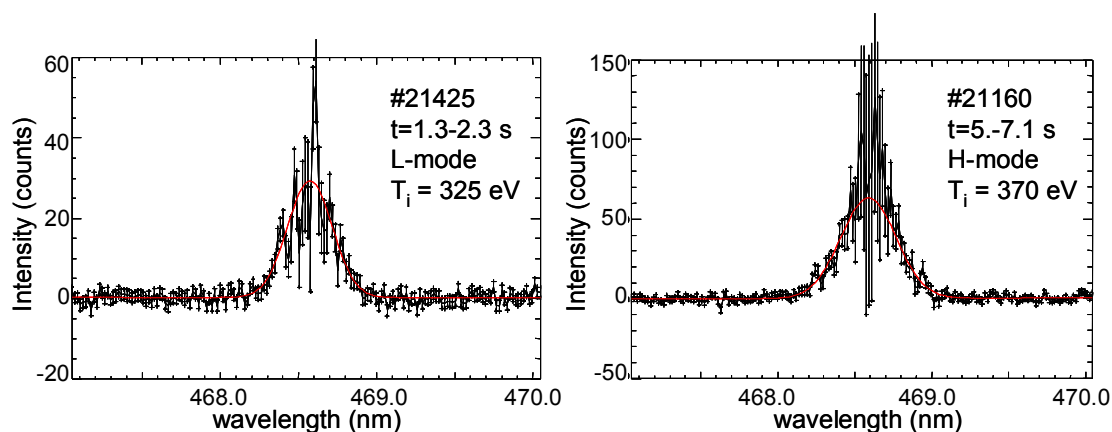


Figure 2: Typical Li-CXS HeII spectra taken with the newly installed EMCCD camera (PhotonMax 512B) for a) an L-mode plasma and b) an H-mode plasma with all frames containing ELMs removed.

The data are fit with a Gaussian to determine the ion temperature. The fit to the spectrally resolved data allows the determination of the otherwise noise dominated line centre. In ELMy H-mode plasmas, the line width and thus also the line intensity is determined by the wings of the Gaussian profile. The measurements are limited to regions with temperatures significantly larger than the He^+ region from where the strong passive line originates.

The intensity derived from the Gaussian fit depends on the impurity ion density n_Z , the charge exchange emission rate $\langle \sigma v_{\text{Li}} \rangle$ and the Lithium beam density n_{Li} . Absolute calibration is achieved by simultaneous beam emission spectroscopy (Li-IXS system). The relative occupation number of $\text{Li}(n/l)$ atoms in the beam is calculated by a beam attenuation

code³ and is temporally and spatially dependent on the plasma electron density and temperature. The atomic data for electron capture from various initial Li(*n*l) states into *n*l-resolved final states of He⁺ have been corrected for collisional mixing when calculating emission cross sections. Taking all errors into account (except from collisional mixing) a systematic error of 20% has to be added to the statistical errors from the measurements. The latter stems from the photon statistics of the charge exchange measurements and the subsequent fit to the measured data. The error variation depends mainly on the impurity ion density and the local current density of the Lithium beam.

Results and Discussion

In the last experimental campaign, He²⁺ ion densities were routinely measured in the ASDEX Upgrade standard ohmic discharges carried out at the beginning of an experimental day and after wall cleaning by a 10 - 20 minute He glow discharge. In the first 20 to 30 discharges after wall boronization the He²⁺ concentration ($n_{\text{He}^{2+}}/n_e$) is found to be between 12 and 15% in the later part of the discharge ($t = 3.4 - 4.5$ s, line integrated density $\sim 4 \cdot 10^{19} \text{ m}^{-3}$). In an earlier part from 1.7 to 2.3 s the discharge has an even lower line integrated density of $2.5 \cdot 10^{19} \text{ m}^{-3}$. Here the concentration rises to 20%, indicating that the He²⁺ impurity ion density stays approximately constant for both density steps ($n_{\text{He}^{2+}} = 4\text{-}5 \cdot 10^{18} \text{ m}^{-3}$). The He²⁺ concentration rises up to 30% in similar discharges later in the boronization cycle. Similar trends are shown with passive spectroscopy of the HeII Ly $_{\alpha}$ line (30.4 nm) measuring the He influx and recycling from the high field side central column⁴. In order to reduce the He content in the plasma, twelve discharges in a row were carried out without conditioning the vessel walls by means of He glow discharges. As can be seen in figure 3, the He²⁺ concentration dropped from around 20% at $\rho_{\text{pol}} = 0.9\text{-}0.95$ for shot #21401 down to 3% for shot #21406. This value stayed constant for the following 4 discharges. The regeneration of the cryo pump caused an increase of the He²⁺ concentration to 5% for shot #21413. With such low He densities, the Li-CXS signal is small and densities can only be evaluated for few LOS.

The radial density profiles (see figure 3a) in the pedestal and edge transport barrier region yield information about impurity transport. First estimates of transport coefficients are derived from STRAHL calculations taking into account the He ionization balance. The maximum of the density distribution of the He⁺ ions is located close to the separatrix, making it difficult to separate between pure transport and effects due to the source. For

radii < 2 cm inside the separatrix, the gradient can only be explained by a negative v/D , i.e. an inward pinch. A similar v/D profile was chosen as in previous impurity transport investigations⁵. The minimum value of -30 m^{-1} , however, differs by more than a factor of 2 from the previous one (-70 m^{-1}) used to model Ne and Si impurity profiles. This could be an indication that the inward convection in the H-mode barrier could depend on impurity charge.

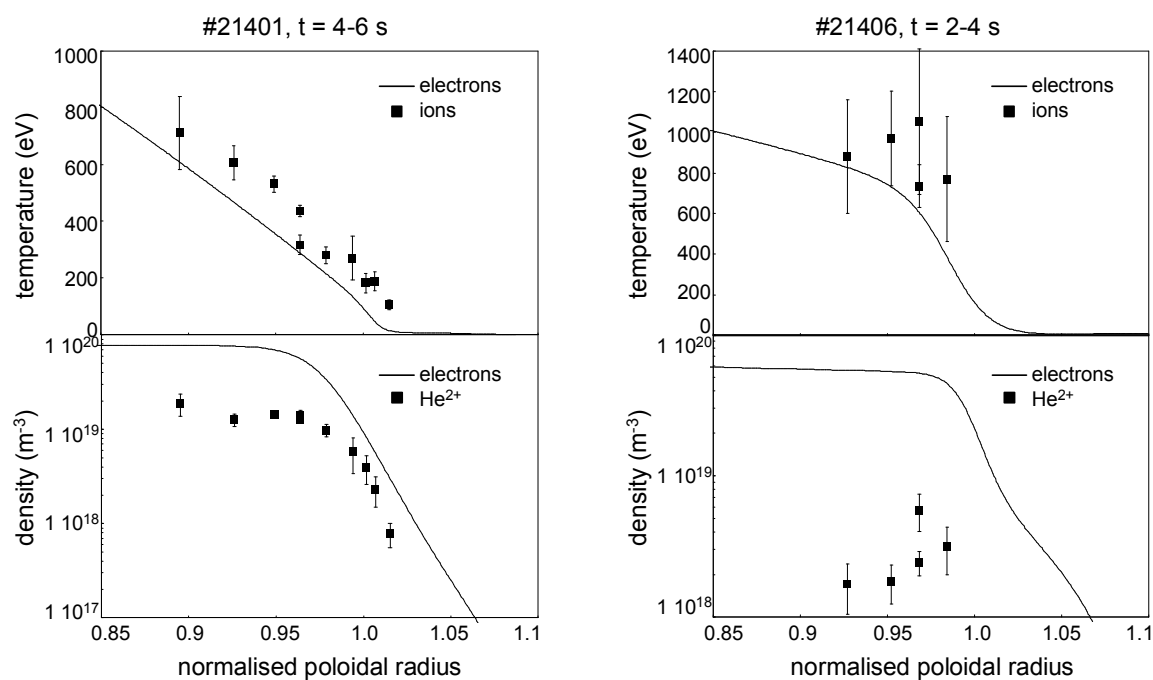


Figure 3: Electron and ion temperatures (upper graph) as well as electron and He^{2+} densities (lower graph) are shown for H-mode discharges #21401 and #21406. The concentration ($n_{\text{He}^{2+}}/n_e$) drops from $\sim 20\%$ down to $\sim 3\%$, because no He glow discharges were carried out in between shots.

Conclusions

Lithium beam charge exchange spectroscopy has been used to determine the He^{2+} concentration at the plasma edge. He glow discharges used for vessel cleaning is the main cause for high He^{2+} concentrations. The He concentration can effectively be reduced by fresh wall boronization as well as by omitting the glow discharges in between shots.

References

- 1 E. Wolfrum et al, Rev. Sci. Instr. 77(3), Art. No. 033507 (2006)
- 2 M. Reich et al, Plasma Phys. Control. Fusion 46, 797-808 (2004)
- 3 R. Brandenburg et al, Plasma Phys. Control. Fusion 41, 471-484 (1999)
- 4 R. Dux, private communication
- 5 R. Dux, Fusion Science and Techn. 44 , 708-713 (2003)